Automatika

Journal for Control, Measurement, Electronics, Computing and Communications

ISSN: (Print) (Online) Journal homepage: https://www.tandfonline.com/loi/taut20

New direct power synergetic-SMC technique based PWM for DFIG integrated to a variable speed dual-rotor wind power

Habib Benbouhenni, Fayçal Mehedi & Lemdani Soufiane

To cite this article: Habib Benbouhenni, Fayçal Mehedi & Lemdani Soufiane (2022) New direct power synergetic-SMC technique based PWM for DFIG integrated to a variable speed dual-rotor wind power, Automatika, 63:4, 718-731, DOI: 10.1080/00051144.2022.2065801

To link to this article: https://doi.org/10.1080/00051144.2022.2065801

Published online: 25 Apr 2022.

AUTOMATIKA
2022, VOL. 63, NO. 4, 718–731
https://doi.org/10.1080/00051144.2022.2065801

Taylor & Francis
Taylor & Francis Group

REGULAR PAPER

New direct power synergetic-SMC technique based PWM for DFIG integrated to a variable speed dual-rotor wind power

Habib Benbouhenni [a], Fayçal Mehedi [b] and Lemdani Soufiane [c]

[a]Faculty of Engineering and Architecture, Department of Electrical & Electronics Engineering, Nisantasi University, Istanbul, Turkey;
[b]Laboratoire Génie Électrique et Energies Renouvelables (LGEER), Faculty of Technology, Hassiba Benbouali University, Chlef, Algeria;
[c]Departement d'électrotechnique, Université de l'USTO-MB, Oran, Algeria

ABSTRACT

In this work, a new direct power synergetic-sliding mode (DPSSM) technique based pulse width modulation (PWM) strategy for doubly-fed induction generator (DFIG) integrated to variable speed dual-rotor wind power (DRWP) systems is designed. The designed strategies produce voltage pulse width locations identical to those of a classical two-level inverter. In this novel control a synergetic-sliding mode (SSM) command and PWM technique to replace the hysteresis comparators and the switching table, for generating the reference voltage using PWM strategies for a classical inverter. Compared with traditional direct active and reactive powers control (DARPC), in this novel strategy, the switching frequency is maintained constant, and the undulations of the reactive power, current, torque, and active power are minimized remarkably. Simulation results verify the validity of the designed strategy.

ARTICLE HISTORY
Received 28 April 2021
Accepted 10 April 2022

KEYWORDS
Direct power synergetic-sliding mode; dual-rotor wind power; pulse width modulation; synergetic-sliding mode control; direct active and reactive powers control

1. Introduction

In a direct power command asynchronous generator's drive, the basic concept is to command both active and reactive powers of the generator simultaneously by the application of two zero voltage vectors and one of the six active full voltage vectors generated by the classical inverter.

The active and reactive powers track their reference values within the limits of two hysteresis bands with two hysteresis controllers and a heuristic switching table to obtain a quick dynamic response [1, 2]. Active power and torque undulations with variable switching operation are the major concerns with a basic DARPC technique [3]. This method is among the most widely used methods in the field of electrical machinery control, especially in the field of wind power generation. The DARPC control method reduces the current and active power ripples compared to indirect vector control (IVC) and direct vector control (DVC). A comparative study between this method and other existing methods is necessary in order to determine the extent of its durability and ease of implementation. Table 1 represents a comparative study between the DARPC method and several methods published in research works, in terms of simplicity, type of user controller, dynamic response, … etc. According to this table, the DARPC method is among the methods that provide better results and are easy to implement compared to other methods. This explains the great use and interest it has received. On the other hand, the operating principle of this method is the same as that of the direct torque control (DTC) method.

In the past decades as reported in works, DARPC based on classical space vector modulation (SVM-DARPC) is one of the most popular solutions for the mitigation of above-mentioned shortcomings of the traditional DARPC technique [4–6]. A constant frequency operation with minimized active and reactive power undulations, but at the expense of increased complexity are the highlights of implementing a DARPC technique with classical SVM technique.

Another approach for active and reactive power undulations reduction is to replace a switching table and hysteresis controllers with an intelligent control (neural networks and fuzzy logic) [7–9]. Availability of more voltage vectors for a given requirement of active and reactive power resulted in an improved response of the technique in terms of active and reactive power undulations but at the cost of enhancement in command complexity and a higher device count. Thus affecting the reliability, simplicity in command, and robustness of the technique which are the key features of a DARPC technique.

In a traditional DARPC technique, increased active and reactive power undulations are also attributed to the application of a single voltage vector for the entire sampling period. These undulations can be easily

CONTACT Habib Benbouhenni habib.benbouenni@nisantasi.edu.tr Faculty of Engineering and Architecture, Department of Electrical & Electronics Engineering, Nisantasi University, 34481742, Istanbul, Turkey

Table 1. A comparative study between DARPC and various published methods.

Criteria	Control techniques						
	DARPC	IVC	DVC	DTC	Backstepping	SMC	SOSMC
Controller	Hysteresis comparators	PI	PI	Hysteresis comparators	–	–	–
Simplicity	Simple	Complicated	Simple	Simple	Complicated	Complicated.	Complicated.
Robustness	++	+	+	++	++++	+++	++++
Response dynamics	Good	Good	Well	Good	Excellent	Excellent	Excellent
Implementation	Easy	Difficult	Easy	Easy	Difficult	Difficult	Difficult
Improvement of transient performance	Good	Weak	Weak	Good	Excellent	Good	Excellent
Reference tracking	+++	++	+	+++	++++	+++	++++

minimized by applying the selected voltage vector-only for a part of the sampling period.

Several solutions have been suggested in order to improve the performance and effectiveness of the DARPC method, for example, sliding mode control (SMC), super twisting algorithm (STA), synergetic control, backstepping control, terminal sliding mode control,… etc. In [10], the DARPC technique was proposed based on integral plus resonant sliding mode controller (IPRSMC) of voltage source converter high voltage direct current (VSC-HVDC) systems. The simulation results showed the robustness of the proposed method compared to the classical method. But, this method is difficult to achieve and this is the negative thing about it. In [11], the DARPC technique was proposed to control the permanent magnet synchronous generator (PMSG) using SMC controller and space vector modulation (SVM), where the traditional switching table was replaced by the SVM technique and two hysteresis controller was replaced by two SMC controllers. The positive of this proposed method is that it is more robust than the classical method and this is what the experimental results show. Another nonlinear method was used in [12] in order to improve the effectiveness of the DARPC method of the DFIG-based wind power. This nonlinear method is adaptive-gain second-order sliding mode control (AGSOSMC). In this work, the author proposed a comparative study between three different methods, namely AGSOSMC-DARPC method, first order sliding mode-DPC (FOSM-DARPC) control technique and FOSM-EDARPC. By observing the results obtained from this work, we find that the THD value for AGSOSMC-DARPC technique is 1.9%, for FOSM-EDARPC control is 2.3% and for FOSM-DARPC method is 5.2%. So the proposed method reduced the THD value by 17.39% and 63.46% compared to FOSM-EDARPC and FOSM-DARPC, respectively. These values indicate the effectiveness of the proposed method in reducing electric current ripples. In [13], the three-level neutral-point-clamped (NPC) inverter is widely used in power conversion due to its simple structure and good characteristics for high-energy. This converter minimized harmonic distortion compared to the conventional converter. In this reference, the authors proposed to use the integral SMC-based DARPC technique to control the NPC inverter and better performances. The DARPC-ISMC method was compared with the DARPC-PI method, the results showed that the DARPC-ISMC method reduced the recovery time by about 25% compared to the DARPC-PI method. A second-order SMC-based DARPC control technique of a DFIG is proposed in [14]. The super twisting algorithm (STA) has been used in [14] to reduce the chattering phenomenon. The designed control technique is a combination of the Lyapunov theory and Thermal Exchange Optimization (TEO), which has been considered to identify the optimal gains of the STA-SOSM controllers. The designed technique (DARPC-STA-SOSM) is compared to the DARPC-PI control strategy in terms of active and reactive power ripples. The simulation results showed that the DARPC-STA-SOSM method reduced the THD value of the rotor and stator current by 62.35% and 63.63%, respectively, compared to the DARPC-PI method. The grid voltage modulated DARPC strategy (GVM-DARPC) for grid-connected voltage source inverters has been proposed in [15]. The GVM-DARPC was proposed to improves the performance of the DARPC control scheme. But, the GVM-DARPC technique gives unsatisfactory results for steady-state performance. In order to improve the steady-state, in this reference, the author suggested the use of the SMC method as a way to improve the performance and effectiveness of the DARPC control strategy. In this work, simulation results and experimental results were almost equal especially in THD value for both GVM-DARPC and GVM-DARPC-SMC methods. In the simulation results, the GVM-DARPC-SMC method reduced the THD value by about 70.44% compared to the GVM-DARPC method and by about 75% in the experimental study. DARPC control scheme with minimum reactive power reference for three-phase AC-to-DC matrix rectifiers using SVM technique is presented [16]. The experimental results show the performances of the designed DARPC strategy. However, the obtained THD of current is 22.30%. In [17], the DARPC control scheme was proposed to control the brushless DC machine using three-phase voltage vector injection. The proposed technique was verified by experimental results. On the other hand, the proposed DARPC technique improves the performances of the brushless DC machine compared to traditional control. In [18], the DARPC control scheme was proposed based on the stator voltage-oriented control principle in which the stator voltage is aligned with the quadrature axis of the rotating reference frame. In [19], three different DARPC algorithm was compared each other in terms of THD value, execution time and settling time of DC voltage. These three types are model predictive DARPC (MP-DARPC), model predictive current control (MPCC) and proportional–integral-based instantaneous current control (PI-ICC). The experimental results show that the MPCC control reduces the THD value compared to MP-DARPC and PI-ICC. On the other hand, the PI-ICC control reduces the execution time compared to MP-DARPC and MPCC. But, the MP-DARPC control reduces the settling time of DC voltage compared to PI-ICC and MPCC. In [20], the zero DARPC was proposed and compared with the traditional DARPC control scheme. The simulation and experimental results show the good performances of the zero DARPC technique compared to the standard DARPC strategy.

In this work, an improvement in the steady-state, as well as dynamic performance of a DARPC technique, is proposed by implementing the DARPC technique, with the following modifications.

(1) An efficient nonlinear controller for reactive and active power undulations minimization.
(2) A robust reactive and active powers command for a fast dynamic response.
(3) A modified SMC controller for the reactive and active powers command loop.

A novel simple reactive and active power undulations minimization strategy with help of a modified SMC technique incorporating an SMC technique by a synergetic control theory is designed for eliminating the reactive and active power undulations and chattering phenomenon.

A DARPC strategy-based synergetic command technique with modified SVM strategy is implemented for active and reactive power command [21] and an SMC command technique is designed to improve the dynamic response of the DFIG-based variable speed dual-rotor wind power (DRWP) systems [22]. Thus this work aims to reduce the active power undulations as well as the effectiveness of the proposed strategy while maintaining the simplicity of technique. The designed technique is illustrated by simulation results.

Summarizing, the novelty and main findings of this paper are as follows:

- A new DARPC control scheme based on the proposed SSM controller is designed to reduce ripples of both reactive and active powers.
- Proposed SSM controllers minimize the tracking error for reactive and active power towards the references of DFIG-based variable speed DRWP systems.
- The DARP-SSM control scheme with PWM technique minimizes harmonic distortion of rotor/stator current and active/reactive ripple of DFIG-based variable speed DRWP systems.

The rest of the paper is organized as follows: An elaborated mathematical model of the DRWP is presented in Section 2. Section 3 presents the proposed nonlinear controller design and stability analysis. In Section 4 the proposed DARPC control scheme with proposed nonlinear controllers is presented. Section 5 shows the comparative simulation results obtained on a 1.5-MW DFIG. Finally, Section 6 provides the conclusions.

2. Model of DRWP

Traditionally, the applied systems of wind turbine systems can be classified into variable speed (VS) and fixed speed turbines (FST). The VS turbine systems (VSTSs) are now more often applied than the systems with FST. The main advantages of VSTSs are: increasing the production of wind power, the ability to achieve maximum power conversion efficiency, and reduction of mechanical stresses.

To this day, there are two types of turbines, which are vertical axis wind turbines and horizontal axis wind turbines. The most widely used is the horizontal axis wind turbine and this is because of the yield it provides compared to the rest of the types. But the problem of this type is that the amount of mechanical energy gained or converted from wind energy remains insufficient. In addition, the effect from neighbouring turbines in the wind farm, where air currents are generated between the turbines, affects the yield. To solve this problem, there is another type of turbine called the multi-rotor wind turbine. In other words, instead of using one turbine, we use several turbines in one turbine. The latter only rotates one generator. The aim of this new turbine is to reduce the effect of unwanted air currents that are produced in the wind farm, As well as raising the value of the mechanical energy gained from the wind.

In this paper, we will use a dual-rotor wind turbine, which is two turbines, one of which is a large turbine, with greater torque, and the other is a small turbine with less torque. On the other hand, the two turbines can be called auxiliary turbine (AR) and main turbine (MR).

The aerodynamic torque of the AT is given [23]:

$$T_A = \frac{1}{2\,\lambda_A^3}.\rho.\pi.R_A^5.C_p.w_A^2 \tag{1}$$

The aerodynamic torque of the MT is given:

$$T_M = \frac{1}{2\,\lambda_M^3}.\rho.\pi.R_A^5.C_p.w_M^2 \tag{2}$$

where λ_A, λ_M: the tip speed ration of the main and auxiliary rotors, R_M, R_A: Blade radius of the auxiliary and main rotors, ρ: the air density and w_A, w_M the mechanical speed of the auxiliary and main rotors.

The tip speed ratios of the AT is given:

$$\lambda_A = \frac{w_A.R_A}{V_1} \tag{3}$$

The tip speed ratios of the MT is given:

$$\lambda_M = \frac{w_M.R_M}{V_M} \tag{4}$$

where, V_M is the speed of the unified wind on main rotor and V_1 is the wind speed on an AWT.

The total aerodynamic torque of DRWP is the AT torque add to the MT torque as shown by the following equation:

$$T_{DRWT} = T_T = T_M + T_A \tag{5}$$

where, T_M is the MT torque, T_A is the AT torque, T_T is the total torque.

The wind speed on the auxiliary and main turbines is the essential element to calculating the tip speed ratio. Equation (6) represents the wind speed in the main turbine [24]. The distance between the main and the auxiliary turbines is 15 metres.

$$V_x = V_1(1 - \frac{1-\sqrt{(1-C_T)}}{2}(1 + \frac{2.x}{\sqrt{1+4.x^2}})) \tag{6}$$

where, *x:* the non-dimensional distance from the auxiliary rotor disk, *Vx*: is the velocity of the disturbed wind between rotors at point x and C_T the trust coefficient, which is taken to be 0.9 [25].

The *Cp* is given:

$$C_p(\lambda,\beta) = \frac{1}{\lambda + 0.08\beta} - \frac{0.035}{\beta^3 + 1} \tag{7}$$

where, β is pitch angle (in this work the $\beta = 0$).

3. Proposed nonlinear controller

SMC is a class of variable structure command it is efficient and robust for linear and nonlinear systems [26]. The main task of the SMC technique is to provide a switching surface, according to laws of existence, convergence, and stability. The switching surface can be reached by the state path through appropriate changes in the structure of the controlled system.

The purpose of the SMC technique is to draw the state path on the sliding surface S (sliding surface) and drag it around it. Once the sliding surface is reached, the dynamics of the system remain insensitive to changes in process parameters and to external disturbances.

The synthesis of control by sliding modes goes through three essential steps [27]:

(1) Choice of the sliding surface,
(2) Establishing the conditions of existence and convergence,
(3) Determine the control law that allows you to reach the surface and stay there.

The choice of sliding surfaces concerns not only the necessary number of surfaces but also their shapes depending on the application and the intended purpose.

The purpose of the command is to keep the surfaces at zero. The latter is a linear differential equation whose unique solution is $e(x) = 0$.

The approach is proven to be important because of several advantages such as:

- Simplicity of design and implementation;
- Independence from variations in the dynamic characteristics of systems;
- Independence from external disturbances;
- The variety of modes of application, in regulation and observation.

Although having various advantages, this command technique also has a disadvantage that limits its use initially. Indeed, in practice, imperfections such as switching delays and hysteresis cause oscillations around the sliding surface.

The major disadvantage of a first-order SMC technique is the chattering effect it generates. The latter can destabilize the closed-loop system and alter the actuator. On the other hand, several techniques have been proposed to reduce this phenomenon [28–32]. We present here another approach suggested in this article, which allows us to minimize the chattering phenomena and improving command strategy.

The command generally includes two terms, a continuous term or base frequency called equivalent command $u_{eq}(t)$ corresponding to the ideal sliding regime (The operating point remains on the surface and the derivative of the surface function remains zero) and a term switching $u_n = -K.\text{sign}(S)$, which forces the operating point to remain in the vicinity of the surface. Equation (8) represents the principle of the SMC method.

$$u(t) = u_{eq}(t) + u_n(t) \tag{8}$$

With:

$$u_n(t) = -K.sign(S) \quad (9)$$

Equation (10) represents the principle of the synergetic command theory.

$$K_1\,\dot{S}(x) + S(x) = 0 \quad (10)$$

The solution of Equation (10) is given by:

$$S(t) = S_0\,e^{t/k1} \quad (11)$$

The proposed nonlinear method is based on replacing the continuous term of the SMC technique with synergetic command (equation (10)), to obtain a more durable method and thus reduce the fluctuations in the active and reactive powers. The suggested method is called the synergetic-sliding mode (SSM) command. It is a combination of SMC techniques and synergetic commands. To have a more durable method and new features. The proposed method is more simple and does not require mathematical calculations compared to other methods. Equation (12) represents the principle of the proposed SSM method.

$$w(t) = -\,K_1\,.sign(S) + K_2\,.\dot{S} + S \quad (12)$$

In this work, we apply this proposed method (SSM) to minimize fluctuations in torque and active power as well as improve the effectiveness of the DARPC control scheme.

The stability condition is given by:

$$S \times \dot{S} \prec 0 \quad (13)$$

4. Direct power synergetic-sliding mode control

The schematic block diagram of the designed DARPC technique with SSM controllers is shown in Figure 1. In the designed scheme an SSM controller, which is explained in Section 3 in detail, is utilized in the active and reactive powers command loop. For active and reactive powers minimization, the traditional switching scheme with limited voltage vectors is replaced by a modified scheme with a larger number of voltage vectors. The details of the novel switching scheme are explained in this section.

The detailed technique of the DARPC command based on an SSM regulator applied to the DFIG-based variable speed DRWP system is modified compared to the DARPC-SVM command since it only requires the measurement of the rotor current and voltages for the estimation of the active and reactive power. The hysteresis comparators and switching table have been replaced by two SSM regulators and the PWM technique.

The reactive and active power estimation block keeps the same form as that established for the classical DARPC command described in [33].

$$\begin{cases} Q_s = -\dfrac{3}{2}\left(\dfrac{Vs}{\sigma.Ls}\cdot\Psi_{r\beta} - \dfrac{Vs.Lm}{\sigma.Ls.Lr}\cdot\Psi_{r\alpha}\right) \\ P_s = -\dfrac{3}{2}\dfrac{Lm}{\sigma.Ls.Lr}\cdot(Vs.\Psi_{r\beta}) \end{cases} \quad (13)$$

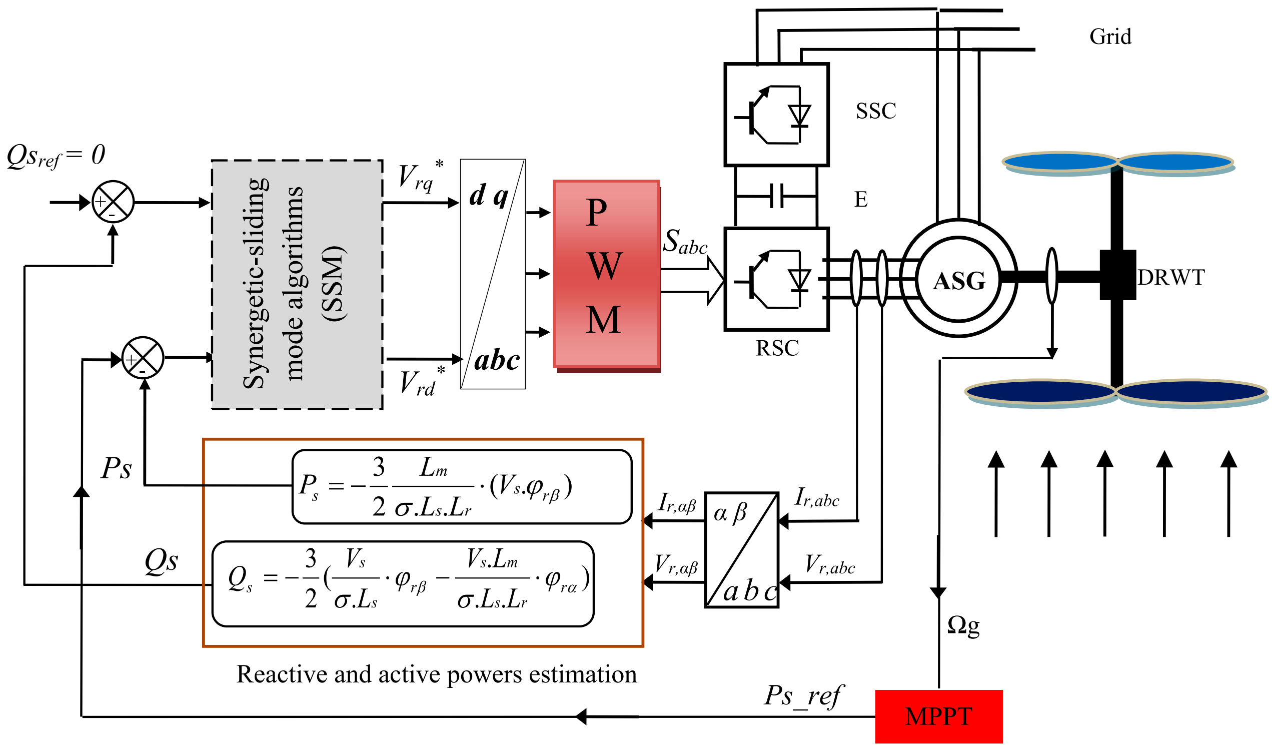

Figure 1. Proposed DRAPC strategy with the SSM controllers.

In this framework, we consider the surfaces defined by equations (14):

$$\begin{cases} S_q = Q_{sref} - Q_s \\ S_p = P_{sref} - P_s \end{cases} \tag{14}$$

Active and reactive powers SSM algorithms are used to influence respectively on the two rotor voltage components as in (15) and (16).

$$V_{qr}^* = -K_1 .sign(S_p(t)) + K_2 \frac{d\, S_p(t)}{dt} + S_p(t) \tag{15}$$

$$V_{dr}^* = -\, K_3 .sign(S_q(t)) + K_4 \frac{d\, S_q(t)}{dt} + S_q(t) \tag{16}$$

Figure 2 shows the internal block diagram of the active and reactive power regulators of the DFIG integrated into a variable speed DRWP system.

This proposed DARPC control scheme (DPSSM) was used to control the DFIG-based variable speed DRWP system. This proposed nonlinear DARPC technique is a simple algorithm, robust method and easy to implement. However, the DPSSM reduced more harmonic distortion and reactive/active power ripples compared to traditional DARPC and other control techniques (Table 2).

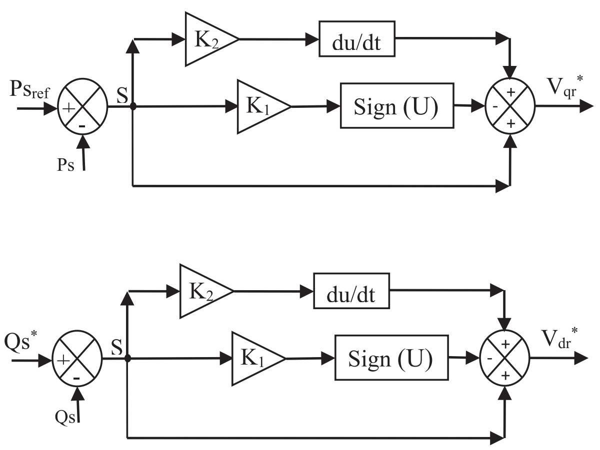

Figure 2. SSM-active and reactive power controllers.

Table 2. Comparative between DPSSM and DARPC control.

Controller	Direct FOC-PI Hysteresis comparator	Direct FOC-SYSTA SSM
Simplicity of calculations	✓	✓
Robustness		✓
Improvement of transient performance		✓
Simplicity of filter design and inverter	✓	✓
Improvement of dynamic response		✓
Negligible parameter effects on system performance		✓
Control inverter	Switching table	PWM

5. Results and discussion

The synergetic-sliding mode command, with the choice of active and reactive powers as sliding surfaces, was validated by numerical simulation using Matlab/Simulink software.

Figures 3–8 show the simulation results obtained relating to this test. According to Figures 5 and 8, we note for the two commands that the power setpoints are followed by those measured by the DFIG-based variable speed DRWP system. In addition, we observe that the DPSSM command has fewer ripples in the curves of the active and reactive power compared to those of the DARPC command (Figures 9 and 10). The reduction can be estimated at 41.17% and 94% for the active and reactive powers, respectively compared to the traditional DARPC method.

The torque of both control techniques is shown in Figure 7. Through this figure and Figure 5, we find that the torque of both control techniques has the same form as the active power, and this appears through the increase and decrease in the value of the torque linked to the increase and decrease in the active power. It can be said that the change in torque is direct with the change in the active power (torque depends directly on the active power). By observing Figure 11, we find that the proposed method (DPSSM) in this work reduced torque ripples, and the reduction rate is estimated at 40% compared to the classical method (DARPC).

The electric current obtained from the two proposed methods is shown in Figure 8. Through this figure, we note that the change in current is related to the change in the active power and wind speed. It can be said that the value of the output current is related to the reference value of the active power for the two methods together. On the other hand, the DPSSM control method gave fewer current ripples than the classical DARPC method (see Figure 12). The ripple reduction can be estimated at 50%.

Figures 3 and 4 illustrate the THD value of the current (Ias) of both command techniques. Note that the value of THD is reduced for DPSSM technique (THD = 0.24%) compared to classical DARPC (THD = 0.53%). It can be said that the proposed control improved the THD value by about 54.47% compared to the traditional DARPC control scheme. Through these results, it is clear that the DPSSM control scheme is much better than the classical method (DARPC), and this is due to the use of the proposed SSM controller. In order to confirm this result reached in this part, we will change the parameters of the DFIG and see the robustness of the proposed DPSSM control scheme compared to the classical DARPC method.

Figures 9–12, illustrate the zooms on the active power, reactive power, torque and stator current of the DFIG-based variable speed DRWP system.

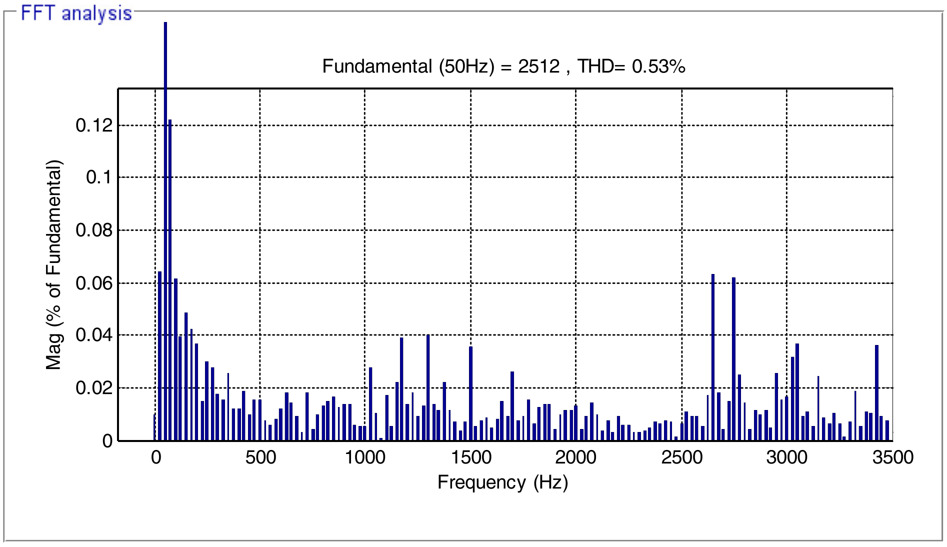

Figure 3. THD (DARPC).

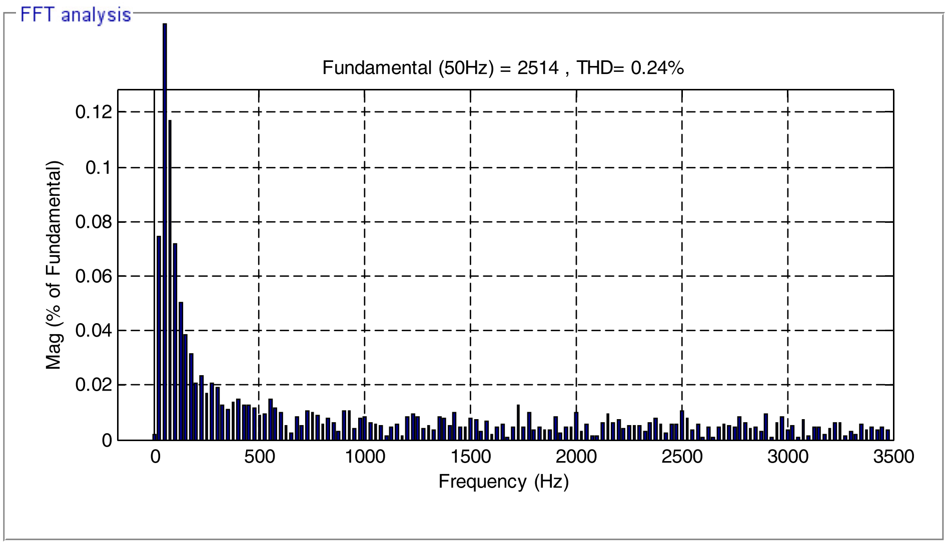

Figure 4. THD (DPSSM).

5.1. Robustness test

The robustness test consists of voluntarily varying the parameters of the model of the DFIG used and seeing the effect of this variation on the responses of the system. The robustness of the two control methods used is tested by the following severe conditions:

- Resistances *Rs*, *Rr* multiplied by 2;
- Inductances *Ls*, *Lm*, and *Lr* multiplied by 0.5.

The simulation results obtained are shown in Figures 13–18. Note for the two types of commands used (DPSSM and DARPC) that the measured powers (active and reactive) follow their references perfectly

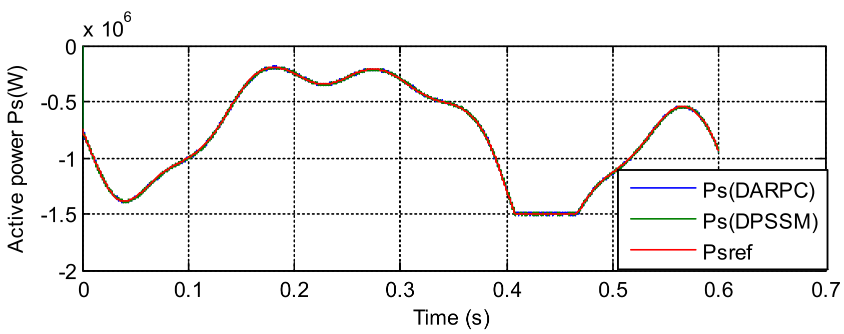

Figure 5. Active power.

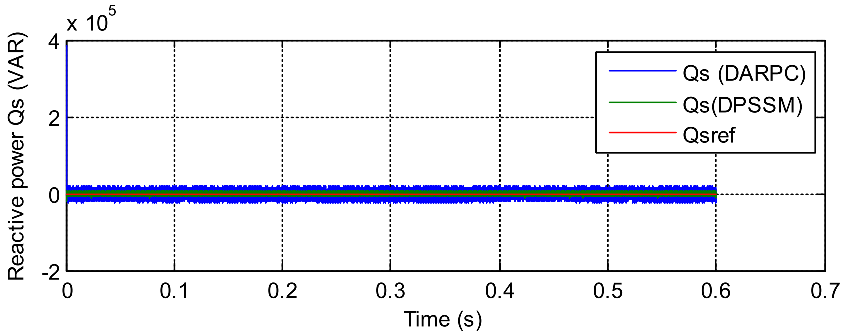

Figure 6. Reactive power.

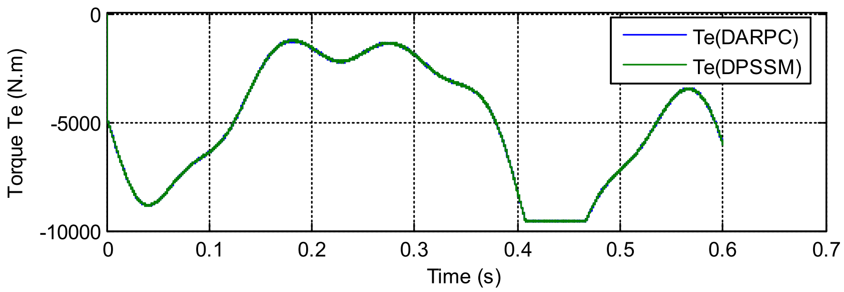

Figure 7. Torque.

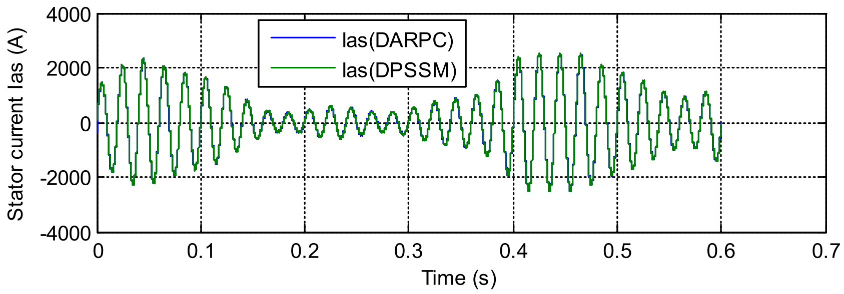

Figure 8. Current (*Ias*).

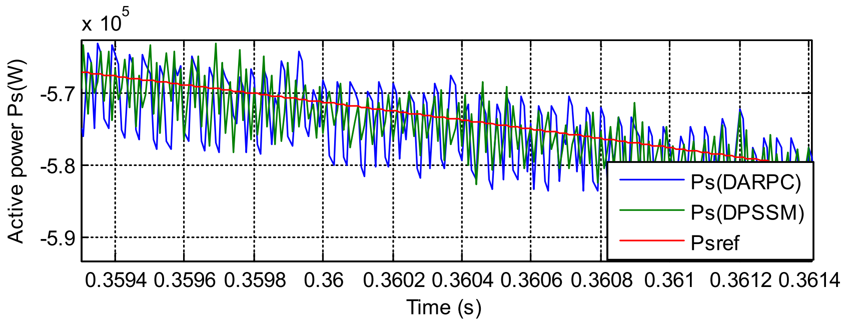

Figure 9. Zoom in the active power.

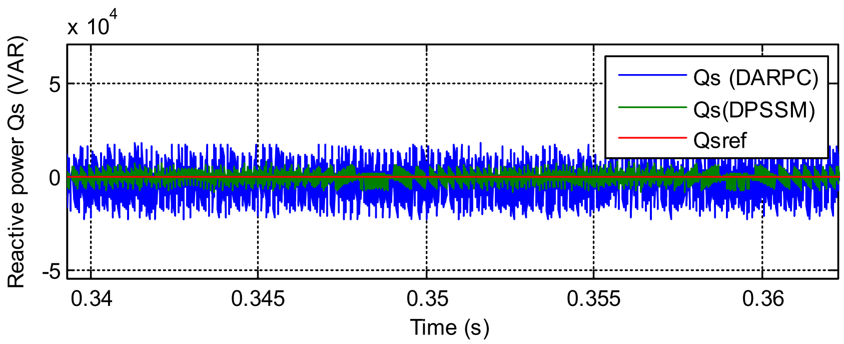

Figure 10. Zoom in the reactive power.

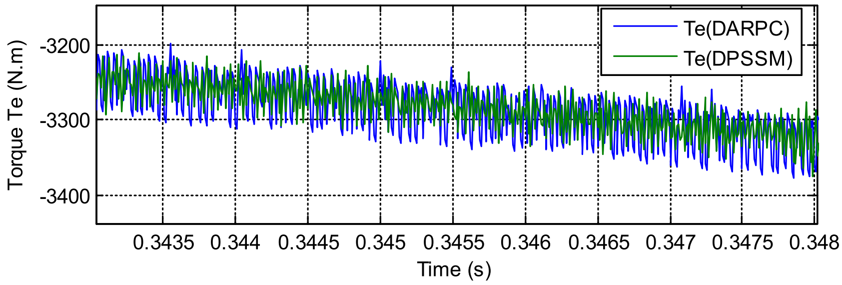

Figure 11. Zoom in the torque.

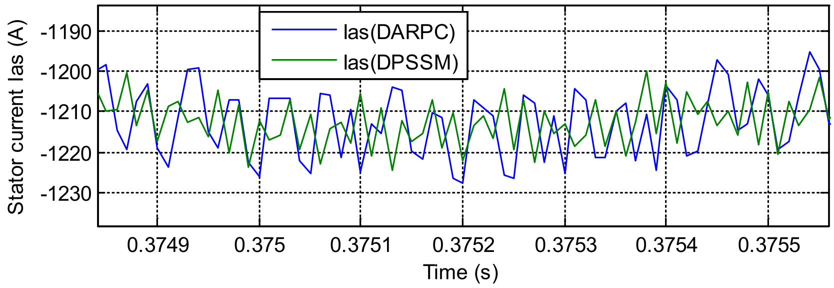

Figure 12. Zoom in thestator current.

(Figures 15–16). Figures 17–18, illustrate successively, the curves of the torques and stator currents of the two types of command such that one notices fewer undulations for the DPSSM compared to the DARPC, appearing in the curves of the two sizes. On the other hand, the DPSSM command reduces the stator current THD value of the DFIG-based variable speed DRWP system (see Figures 13 and 14). In Table 3, we summarize the performances and characteristics of the two control methods used, noted in the simulation results. Therefore, the DPSSM-DFIG system ensures a good quality of power supplied to the receiver (network or load) (Figures 19–22).

The DPSSM strategy can be compared with the DARPC control scheme from several aspects, for example, the dynamic response, simplicity, the value of reactive power ripples, … etc. Table 4 shows a comparative study between the DPSSM strategy and the DARPC control scheme, according to the results obtained from the numerical simulation. It is clear that the DPSSM strategy is more robust than the DARPC control scheme except for the rise time, dynamic response, settling time, overshoot which is faster in the DPSSM strategy than the DARPC control scheme. On the other hand, the DPSSM strategy provided better results in terms of active power ripples, active and reactive power tracking, and the quality of the produced stator current.

In the end, we study a comparison between the DPSSM technique and several published papers in

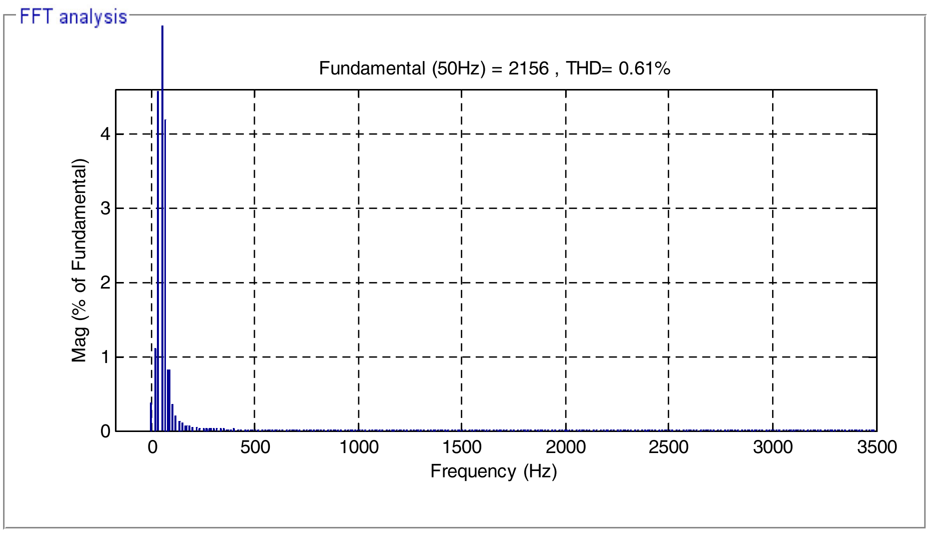

Figure 13. THD of stator current (DARPC).

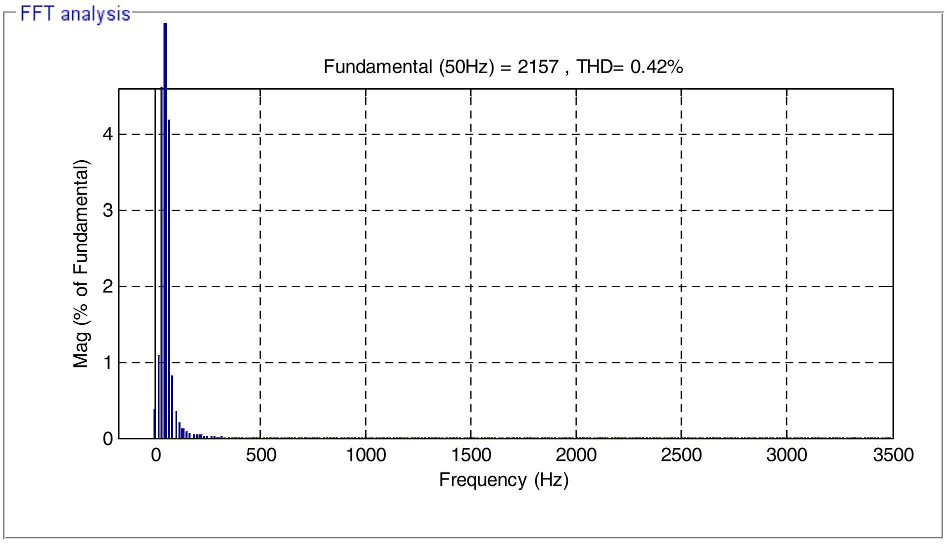

Figure 14. THD of stator current (DPSSM).

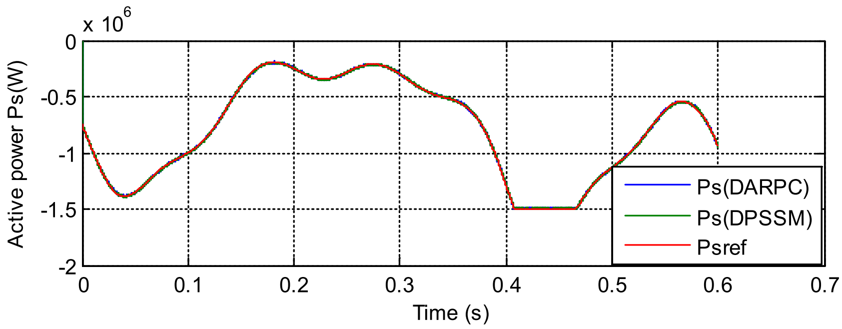

Figure 15. Active power.

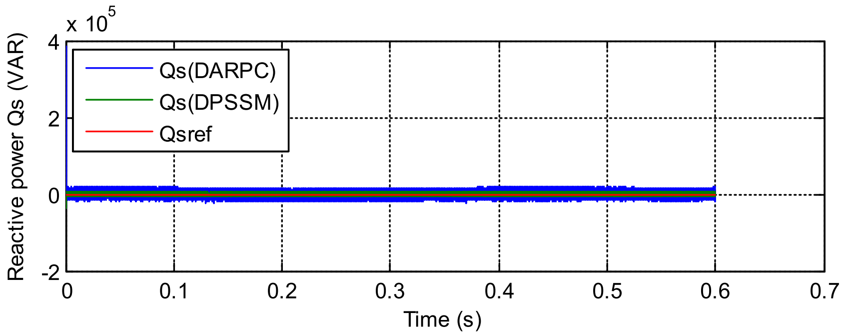

Figure 16. Reactive power.

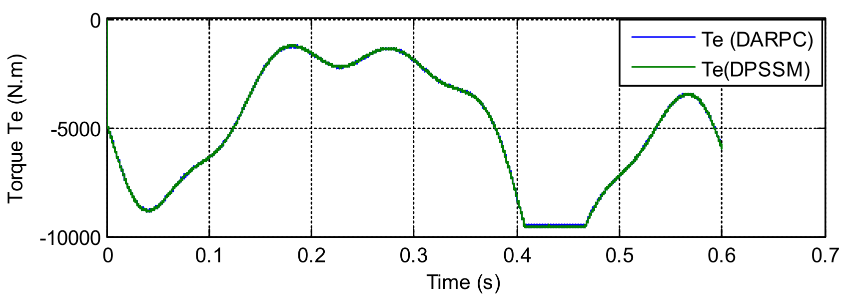

Figure 17. Torque.

terms of the percentage of the THD of stator current. The results are recorded in Table 5. Through this table, we note that the DPSSM technique gave much lower percentages of the THD than some of the published strategies such as FOC, DTC, and fuzzy DTC control. So, it can be said that the DPSSM technique in this paper gives a sinusoidal current that has good characteristics in terms of ripples

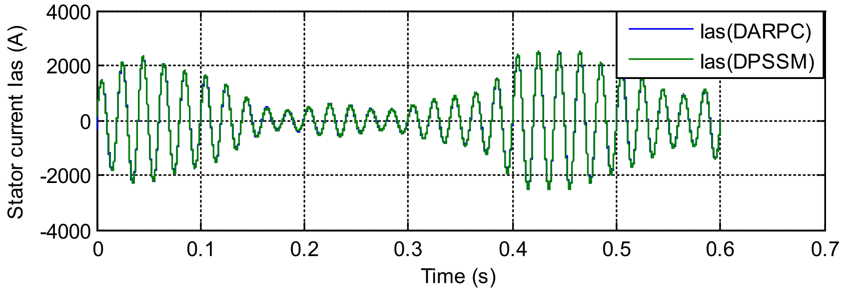

Figure 18. Current.

Table 3. Characteristics of both strategies.

	DARPC	DPSSM
THD (Ias)	0.61%	0.42%
Reactive and active power reduction	−	+
Durability	−	+
Simplicity	+	+
Quality of stator current	−	+

Table 4. Compare the results obtained from the DPSSM with the DARPC control.

	Strategies	
Criteria	DARPC	DPSSM
Reactive and active power tracking	Good	Excellent
THD (%)	0.53	0.24
Dynamic response (s)	Medium	Fast
Settling time (ms)	High	Medium
Reduce active and reactive power ripples	Acceptable	Excellent
Overshoot (%)	Remarkable ≈ 21%	Neglected ≈ 1%
Simplicity of converter and filter design	Simple	Simple
Active power: ripple (W)	Around 17,000	Around 5000
Sensitivity to parameter change	High	Medium
Torque: ripple (N.m)	Around 100	Around 60
Rise time (s)	High	Medium
Simplicity of calculations	Simple	Rather complicated
Reactive power: ripple (VAR)	Around 20000	Around 1100
Stator current: ripple (A)	Around 25	Around 11
Improvement of transient performance	Good	Excellent
Quality of stator current	Acceptable	Excellent

Table 5. Summary table of results obtained compared to other control techniques.

Reference	Strategy	THD (%)
Ref. [34]	DTC control	2.57
	Fuzzy DTC control	
Ref. [4]	FOC control	3.7
Ref. [35]	DARPC with IP controllers	0.43
Ref. [36]	12 sectors DARPC(12-DARPC) control	0.40
Ref. [37]	Fuzzy SMC method	1.15
Ref. [38]	SOSMC method	3.13
Ref. [29]	DARPC control with STA controller	1.66
Ref. [4]	FOC with neuro-fuzzy controller (FOC-NFC)	0.78
	FOC with Type 2 fuzzy logic controller (FOC-T2FLC)	1.14
Ref. [39]	Integral sliding mode control (ISMC)	9.71
	Multi-resonant-based sliding mode controller (MRSMC)	3.14
Ref. [40]	DARPC with terminal synergetic controller	0.25
Ref. [41]	Direct FOC control	2.94
	Direct FOC with third-order sliding mode	1.42
Ref. [42]	Direct FOC control	1.45
	Direct FOC with synergetic-sliding mode	0.50
Proposed control methods	DARPC control	0.53
	DPSSM control	0.24

and THD value compared to the rest of the published strategies, and this is what makes the life of the devices longer and minimizes the cost of maintenance.

6. Conclusion

This work has been devoted to the study and application of the DARPC command technique with the SSM controllers and compared to that equipped with conventional hysteresis comparators.

Through numerical simulation results, we have shown the efficiency of the adopted command (DPSSM) especially in the attenuation of the undulations at the power levels due to the elimination of the hysteresis regulators and the improvement of the screw robustness. For the parametric variations and the attenuation of the chattering phenomenon.

The DPSSM command provides an improvement over the DARPC technique. This improvement is remarkable especially in the value of THD of stator currents and the responses of powers and torque. The THD reduction can be estimated at 54.71%. Therefore, it makes it possible to limit the undulations at the level of different electrical quantities. The reduction ratios were about 70%, 40%, 56% and 95% for active power, torque, current and reactive power, respectively. Observing these percentages, we find that they are high, which indicates the robustness of the proposed method to improve the performance of the DFIG-based variable speed DRWP system. But, it cannot completely eliminate them. So for a more satisfactory improvement, we will try in the next work to take advantage of the advantages of one of the techniques based on artificial intelligence to further improve the performance of the DPSSM-DFIG system.

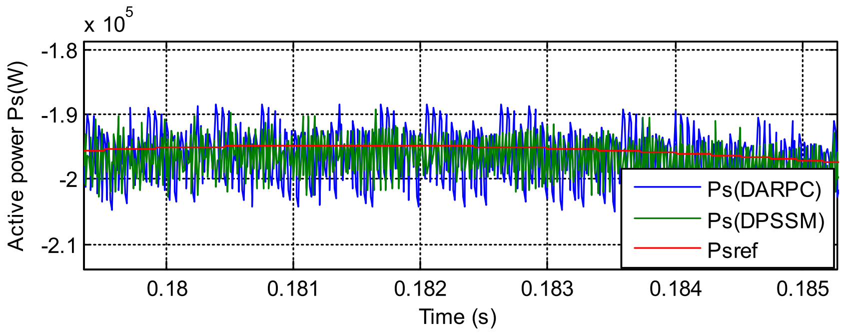

Figure 19. Zoom in the active power.

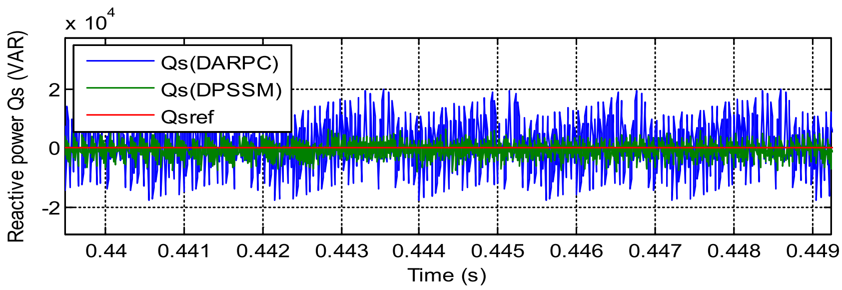

Figure 20. Zoom in the reactive power.

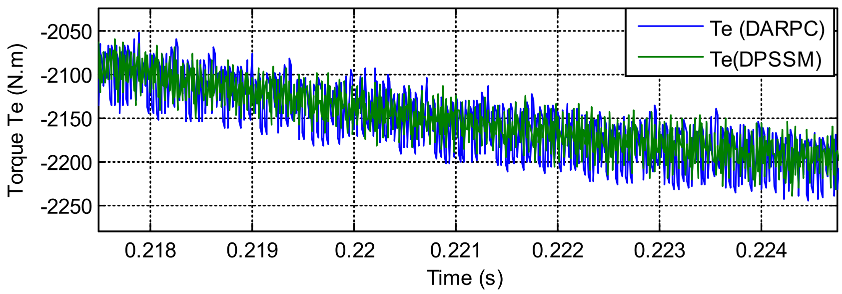

Figure 21. Zoom in the torque.

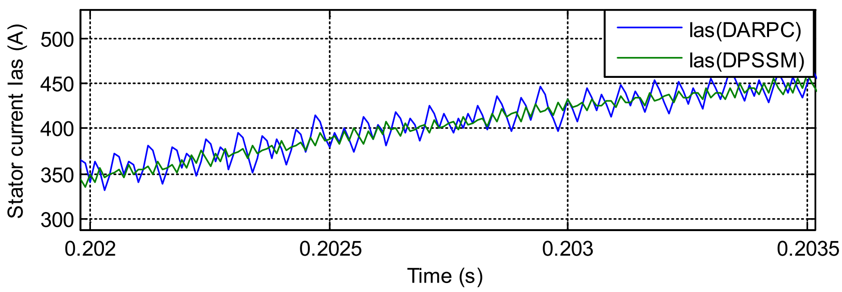

Figure 22. Zoom in the current (Ias).

The current injected into the grid has a low THD value, being equal to 0.24%. The designed DARPC control scheme presents lower current, torque, active power, and reactive power ripples of the DFIG-based variable speed DRWP system.

Summarizing, the main findings of this research are as follows:

- A new synergetic-sliding mode controller was presented and confirmed with numerical simulation.
- A new DARPC control scheme based on a synergetic-sliding mode controller was presented and confirmed with numerical simulation.
- Minimize the harmonic distortion value of rotor/stator current.

- Minimizes the electromagnetic torque, and reactive power, rotor current, and active power ripples.
- A robust control scheme was proposed.

In a future papers, to improve the quality of the rotor/stator current and active power, the DFIG will be controlled using other proposed nonlinear strategies, such as intelligent third-order sliding mode control, fast terminal synergetic control and terminal super twisting algorithm.

Disclosure statement

No potential conflict of interest was reported by the author(s).

ORCID

Habib Benbouhenni http://orcid.org/0000-0001-8253-4863
Fayçal Mehedi http://orcid.org/0000-0002-7527-6859
Lemdani Soufiane http://orcid.org/0000-0003-0372-7507

References

[1] Mirzakhani A, Ghandehari R, Davari SA. A new DPC-based control algorithm for improving the power quality of DFIG in unbalance grid voltage conditions. Int J Renew Energy Res. December 2018;8(4):2229–2238.
[2] Massoum S, Meroufel A, Massoum A, et al. A direct power control of the doubly-fed induction generator based on the SVM strategy. Elektroteh Vestn . 2019;45(5):235–240.
[3] Nian H, Song Y. Direct power control of doubly fed induction generator under distorted grid voltage. IEEE Trans Power Electr. Feb. 2014;29(2):894–905. DOI:10.1109/TPEL.2013.2258943.
[4] Amrane F, Chaiba A. A novel direct power control for grid-connected doubly fed induction generator based on hybrid artificial intelligent control with space vector modulation. Rev Sci Techn Electrotechn Et Energ. 2016;61(3):263–268.
[5] Zhi D, Xu L. Direct power control of DFIG with constant switching frequency and improved transient performance. IEEE Trans Energy Convers. 2007;22(1): 110–118.
[6] Monfared M, Rastegar H, Kojabadi HM. A simple and efficient control strategy for four-switch three-phase power converters. Adv Electr Comp Eng. 2010;10(1): 54–58. DOI:10.4316/AECE.2010.01009.
[7] Heydari E, Rafiee M, Pichan M. Fuzzy-genetic algorithm-based direct power control strategy for DFIG. Iran J Electr Electr Eng. 2018;14(4):353–361.
[8] Bouafia A, Krim F, Gaubert J. Fuzzy-logic-based switching state selection for direct power control of three-phase PWM rectifier. IEEE Trans Indus Electr. June 2009;56(6):1984–1992. DOI:10.1109/TIE.2009.2014746.
[9] Benbouhenni H, Boudjema Z, Belaidi A. Power control of DFIG in WECS using DPC and NDPC-NPWM methods. Math Modell Eng Probl. 2020;7(2):223–236.
[10] Yang W, Zhang A, Li J, et al. Integral plus resonant sliding mode direct power control for VSC-HVDC systems under unbalanced grid voltage conditions. Energies. 2017;10; DOI:10.3390/en10101528.
[11] Zoghlami M, Kadri A, Bacha F. Analysis and application of the sliding mode control approach in the variable-wind speed conversion system for the utility of grid connection. Energies. 2018;11; DOI:10.3390/en11040720.
[12] Han Y, Ma R. Adaptive-gain second-order sliding mode direct power control for wind-turbine-driven DFIG under balanced and unbalanced grid voltage. Energies. 2019;12; DOI:10.3390/en12203886.
[13] Lin H, Leon JI, Luo W, et al. Integral sliding-mode control-based direct power control for three-level NPC converters. Energies. 2020;13; DOI:10.3390/en13010227.
[14] Mazen Alhato M, Bouallègue S, Rezk H. Modeling and performance improvement of direct power control of doubly-fed induction generator based wind turbine through second-order sliding mode control approach. Mathematics. 2020;8; DOI:10.3390/math8112012.
[15] Gui Y, Xu Q, Blaabjerg F, et al. Sliding mode control with grid voltage modulated DPC for voltage source inverters under distorted grid voltage. CPSS Trans Power Electr Appl. 2019;4(3):244–254.
[16] Kim J, Kwak S. Direct power control method with minimum reactive power reference for three-phase AC-to-DC matrix rectifiers using space vector modulation. IEEE Access. 2019;7:67515–67525. DOI:10.1109/ACCESS.2019.2918571.
[17] Wei J, Liu P, Tao W. An incorporated control strategy of commutation and conduction torque ripples mitigation for BLDCM drives in household appliances. IEEE Access. 2019;7:108137–108151. DOI:10.1109/ACCESS.2019.2932837.
[18] Mossa AM, Echeikh H, Diab AAZ, et al. Effective direct power control for a sensor-less doubly fed induction generator with a losses minimization criterion. Electronics. 2020;9; DOI:10.3390/electronics9081269.
[19] Kang L, Zhang J, Zhou H, et al. Model predictive current control with fixed switching frequency and dead-time compensation for single-phase PWM rectifier. Electronics. 2021;10; DOI:10.3390/electronics10040426.
[20] Djazia K, Krim F, Chaoui A. Active power filtering using the ZDPC method under unbalanced and distorted grid voltage conditions. Energies. 2015;8:1584–1605. DOI:10.3390/en8031584.
[21] Shehata EG. Sliding mode direct power control of RSC for DFIGs driven by variable speed wind turbines. Alexandr Eng J. 2015;54:1067–1075.
[22] Djamel Eddine K, Mezouar A, Boumediene L, et al. A comprehensive review of LVRT capability and sliding mode control of grid-connected wind-turbine-driven doubly fed induction generator. Automatika. 2016;57(4):922–935. DOI:10.7305/automatika.2017.05.1813.
[23] Benbouhenni H, Boudjema Z, Belaidi A. Comparison study between neural STSM and ANFIS-STSM method in DPC control scheme of DFIG-based dual-rotor wind turbines. Int J Math Comp Simul. 2020;14:73–86.
[24] Yahdou A, Djilali AB, Boudjema Z, et al. Improved vector control of a counter-rotating wind turbine system using adaptive backstepping sliding mode. J Eur Syst Autom. October, 2020;53(5):645–651.
[25] Yahdou A, Hemici B, Boudjema Z. Sliding mode control of dual rotor wind turbine system. Med J Meas Contr. 2015;11(2):412–419.
[26] Utkin V. Variable structure systems with sliding modes. IEEE Trans Autom Contr. April 1977;22(2):212–222. DOI:10.1109/TAC.1977.1101446.

[27] Feng Y, Yu X, Han F. On nonsingular terminal sliding-mode control of nonlinear systems. Automatica. June 2013;49(6):1715–1722.
[28] Kairus D, Wamkeue R, Belmadani B, et al. Variable structure control of DFIG for wind power generation and harmonic current mitigation,". Adv Electr Comp Eng. 2010;10(4):167–174. DOI:10.4316/AECE.2010.04027.
[29] Yaichi I, Semmah A, Wira P, et al. Super-twisting sliding mode control of a doubly-fed induction generator based on the SVM strategy. Period Polytech Electr Eng Comp Sci. 2019;63(3):178–190.
[30] Benbouhenni H. Sliding mode with neural network regulateur for DFIG using two-level NPWM strategy. Iran J Electr Electr Eng. 2019;15(3):411–419.
[31] Rezaei MM, Soltani J. Sliding mode control of a grid-connected distributed generation unit under unbalanced voltage conditions. Automatika. 2016;57(1):89–98. DOI:10.7305/automatika.2016.07.870.
[32] Luo H, Zheng J. Dissipativity-based fuzzy integral sliding mode control of nonlinear stochastic systems. Hind Discr Dyn Nature Soc. 2021;2021:1–12. DOI:10.1155/2021/6650516.
[33] Xu L, Cartwright P. Direct active and reactive power control of DFIG for wind energy generation. IEEE Trans Energy Convers 2006;21(3):750–758.
[34] Ayrira W, Ourahoua M, El Hassounia B, et al. Direct torque control improvement of a variable speed DFIG based on a fuzzy inference system. Math Comput Simul. 2020;167:308–324. DOI:10.1016/j.matcom.2018.05.014.
[35] Fayssal A, Bruno F, Azeddine C. Experimental investigation of efficient and simple wind-turbine based on DFIG-direct power control using LCL-filter for stand-alone mode. ISA Trans. 2021: 1–34. in press. DOI:10.1016/j.isatra.2021.07.008.
[36] Benbouhenni H. Twelve sectors DPC control based on neural hysteresis comparators of the DFIG integrated to wind power. Tecnica Italiana. 2020;64(2):223–236.
[37] Boudjema Z, Meroufel A, Djerriri Y, et al. Fuzzy sliding mode control of a doubly fed induction generator for energy conversion. Carpath J Electr Comp Eng. 2013;6(2):7–14.
[38] Yahdou A, Hemici B, Boudjema Z. Second order sliding mode control of a dual-rotor wind turbine system by employing a matrix converter. J Electr Eng. 2016;16(3):1–11.
[39] Quan Y, Hang L, He Y, et al. Multi-resonant-based sliding mode control of DFIG-based wind system under unbalanced and harmonic network conditions. Appl Sci. 2019;9; DOI:10.3390/app9061124.
[40] Benbouhenni H, Bizon N. Terminal synergetic control for direct active and reactive powers in asynchronous generator-based dual-rotor wind power systems. Electronics. 2021;10(16):1–23. DOI:10.3390/electronics10161880.
[41] Benbouhenni H, Bizon N. Third-order sliding mode applied to the direct field-oriented control of the asynchronous generator for variable-speed contra-rotating wind turbine generation systems. Energies; 14(16):1–20. DOI:10.3390/en14185877.
[42] Benbouhenni H, Bizon N. A synergetic sliding mode controller applied to direct field-oriented control of induction generator-based variable speed dual-rotor wind turbines. Energies. 2021;14(15):1–17. DOI:10.3390/en14154437.